Superconducting Pb Island Nanostructures Studied by Scanning Tunneling Microscopy and Spectroscopy

Takahiro Nishio,[1] Toshu An,[1,*] Atsushi Nomura,[1,+] Kousuke Miyachi,[1] Toyoaki Eguchi,[1] Hideaki Sakata,[2] Shizeng Lin,[3] Nobuhiko Hayashi,[4] Noriyuki Nakai,[4] Masahiko Machida,[4] and Yukio Hasegawa[1,‡]

[1]*The Institute for Solid State Physics, The University of Tokyo, Kashiwa-no-ha, Kashiwa, 277-8581, Japan*
[2]*Department of Physics, Tokyo University of Science, Shinjuku-ku, Tokyo 162-8601, Japan*
[3]*WPI Center for Materials Nanoarchitectonics, National Institute for Materials Science, Tsukuba 305-0047, Japan*
[4]*CCSE, Japan Atomic Energy Agency, and CREST, Japan Science and Technology Agency, Higashi-ueno, Taito-ku, Tokyo, 110-0015, Japan*

(Received 8 March 2008; published 14 October 2008)

Superconductivity of nanosized Pb-island structures whose radius is 0.8 to 2.5 times their coherence length was studied under magnetic fields using low-temperature scanning tunneling microscopy and spectroscopy. Spatial profiles of superconductivity were obtained by conductance measurements at zero-bias voltage. Critical magnetic fields for vortex penetration and expulsion and for superconductivity breaking were measured for each island. The critical fields depending on the lateral size of the islands and existence of the minimum lateral size for vortex formation were observed.

DOI: 10.1103/PhysRevLett.101.167001 PACS numbers: 74.78.Na, 68.37.Ef, 74.78.Db, 74.81.Bd

Mesoscopic superconductors, whose sizes are of the order of their coherence length, exhibit properties significantly different from those of their bulk counterparts. In bulk superconductors, the penetrating vortices form a triangular Abrikosov lattice. On the other hand, small superconductors exhibit various states of vortices, such as a giant vortex [1,2] and an antivortex [3], depending on their size and shape. These unique features have been observed experimentally by electrical conductance and magnetization measurements. Using low-temperature (LT) scanning tunneling microscopy or spectroscopy (STM/S), the Abrikosov lattice was observed by Hess *et al.* [4,5]. In the present study, we investigated size-dependent superconductivity of nanosized materials through local measurements of superconductivity and its imaging using LT-STM/S.

As samples, we used (111)-oriented single-crystalline Pb-island structures formed on a Si (111) substrate, whose radii were 25–75 nm and thickness was 3 nm. Growth of Pb on the substrate has been studied intensively because of its unique quantum size effect [6] and subsequent electronic growth [7]. Since Pb is one of the elemental superconductors with high critical temperature (T_c, 7.2 K), superconductivity of Pb films and islands has been studied. Various interesting phenomena, for instance, oscillatory transition temperature with thickness [8–10], island-size-dependent superconductivity [11], and vortex pinning at void structures in thin films [12], have been reported. In this study, we investigated superconductivity of Pb islands and their size effect under magnetic fields. To avoid unwanted effects caused by contaminations or capping layers, we prepared samples, characterized their sizes and shapes from STM images, and measured their superconductivity by tunneling spectroscopy *in situ* under ultrahigh vacuum conditions.

A ^{3}He-cooled LT-STM (Unisoku, USM-1300S with a Nanonis controller), whose lowest temperature is 0.5 K, was used for this study [11]. It can be operated under magnetic fields of up to 7 T perpendicular to the sample surface. The samples were prepared by Pb deposition on a cooled (200–240 K) (7×7)-reconstructed Si(111) substrate (As doped, 1–3 mΩ cm) and subsequent annealing at $\sim$300 K for 30 min to flatten the island tops. By controlling the deposition temperature we adjusted the size of the islands; lower temperature deposition produces smaller islands. All STM/S measurements were performed at 2.0 K with a tungsten probe tip after cooling the sample under zero magnetic field. An oxide layer covering the tip was removed by field evaporation using *in situ* field ion microscopy prior to the measurements.

A typical Pb island is shown in Fig. 1(a). Its thickness was uniform and estimated at 9 monolayers (MLs, 1 ML = 0.286 nm) excluding a wetting layer from a height measurement of the STM image. According to Özer *et al.* [12], the coherence length ξ and the penetration depth λ of the 9-ML Pb thin film on the substrate at 2 K are 30 and 150 nm, respectively. Since ξ of thin films is limited by the thickness due to surface/interface scattering [13], ξ of the 9-ML islands is safely assumed to be that of the thin film. Therefore, the lateral size of the island is a few times larger than ξ, but smaller than λ, whereas its thickness is considerably smaller than the two characteristic lengths.

Tunneling spectra taken under various magnetic fields at the center of the island (A) and a peripheral site (B, 40 nm from A) are shown in Figs. 1(b) and 1(c), respectively. In zero magnetic field, the spectra taken at both sites are the same, as observed in our previous study [11]. In contrast, under nonzero magnetic fields, the spectra depend on the sites. At 0.6 T, the superconducting gap at A almost disappears, whereas the gap at B does not. The gap disappear-

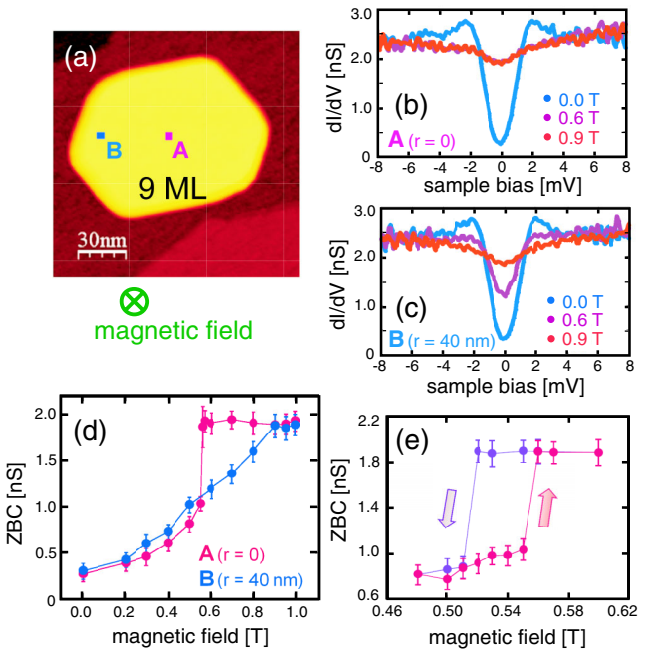

FIG. 1 (color online). (a) STM image of a 9 ML Pb island. (b), (c) Tunneling spectra showing a superconducting gap measured at the center A (b) and a peripheral site B (40 nm from A) (c) under various magnetic fields perpendicular to the island. (d) Plot of zero-bias conductance (ZBC) measured under various magnetic fields. (e) ZBC plot measured at A near the magnetic field where the ZBC jumps at the island center.

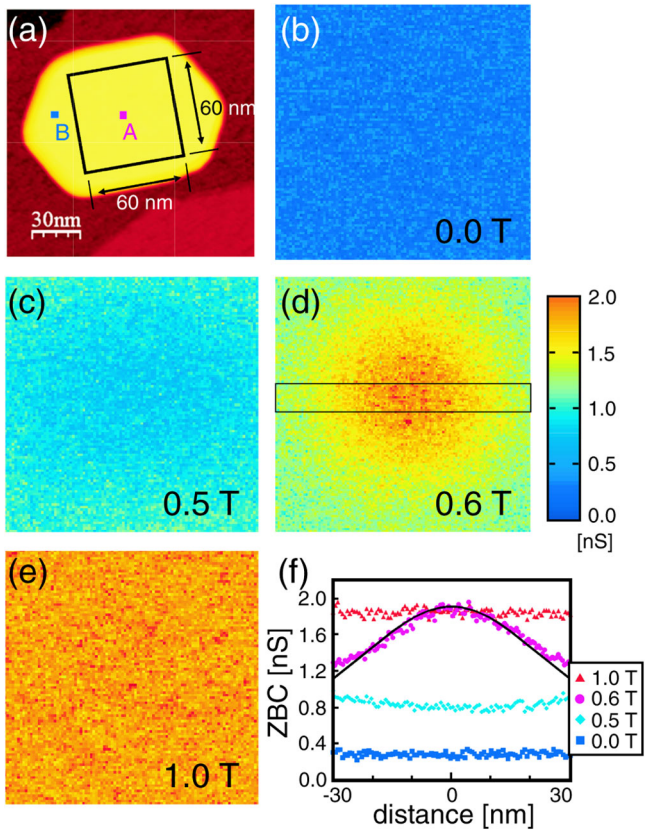

FIG. 2 (color online). (a) STM image of a Pb island, same as that in Fig. 1, showing an area where the following ZBC images were taken. (b)–(e) ZBC images taken under magnetic fields of 0.0 T (b), 0.5 T (c), 0.6 T (d), and 1.0 T (e). (f) Cross-sectional ZBC profiles averaged in the rectangular area shown in Fig. 2(d). The calculated profile of local density of states at the Fermi level for a vortex is also drawn with a solid line.

ance is due to Cooper-pair breaking. Therefore, the tunneling conductance at the zero-bias voltage (zero-bias conductance: ZBC) is an appropriate parameter for characterizing the breakdown of the superconductivity [9]. In the following experiments, we measured the ZBC to characterize the superconductivity.

In order to clarify the observed site dependence, we measured the variation of the ZBC as a function of the magnetic field [Fig. 1(d)]. The ZBC at B increases monotonically with the field until saturation at 0.9 T, whereas the ZBC at A jumps around 0.6 T up to the saturated value. Since the saturated conductance is close to that outside the superconducting gap, we presume that it indicates complete breakdown of superconductivity. In fact, the saturated ZBC is slightly less than the outside conductance as dip structures are observed in dI/dV spectra taken at 0.9 T [Figs. 1(b) and 1(c)]. This is probably due to the existence of the wetting layer under the Pb islands, since similar dip spectra are also observed on the layer. Figure 1(e) shows the ZBC variation near the jump, that is, a transition magnetic field. The magnified plot indicates hysteresis around the field; the transition field depends on the sweep direction.

To elucidate the observed spatial variation of the ZBC, we recorded images of the ZBC under various magnetic fields in a square area shown in Fig. 2(a). At zero field, the ZBC is small and homogenous in the area. At 0.5 T, the ZBC increases, and moreover, the ZBC in the periphery is slightly larger than that in the center, as more clearly shown in its cross-sectional plot in Fig. 2(f). The large ZBC in the periphery can be attributed to the Cooper-pair breaking due to field penetration. At 0.6 T, which is just above the transition field, the center has a saturated ZBC, while the periphery has a lower ZBC. Then, at 1.0 T, the entire area has a saturated ZBC, indicating complete breakdown of superconductivity in the entire area.

A high ZBC, i.e., breakdown of superconductivity, around the island center observed at 0.6 T implies a vortex formation. In order to confirm the attribution, we calculated the spatial distribution of local density of states (LDOS) at the Fermi level by solving the Eilenberger equation for a two-dimensional superconducting state whose vorticity is equal to 1 [14,15]. The parameters used in the calculations are mean free path and BCS coherence length, which are 9 nm (=3.5 times the thickness) and 98 nm, respectively, as T_c of the 9 ML thin film is 6.1 K [12]. Figure 2(f) shows a comparison of the calculated LDOS with the experimentally obtained ZBC profile,

averaged in a rectangular area of Fig. 2(d), and their good correlations. The observed hysteresis also supports for the vortex formation, since penetration or expulsion of a vortex requires overcoming the Bean-Livingston barrier [16] that exists in the periphery of the island. It should be noted that there is no zero-bias peak originating from the bound state at the vortex center, which was observed on a cleaved $NbSe_2$ surface [5]. The absence of the bound state is due to a short mean free path restricted by its small thickness. Visualization of vortex formation and the breakdown of superconductivity by STM/S allow us to determine various critical fields: H_{p1} (H_{ex1}) for vortex penetration (expulsion), and H_{SN} for the complete breakdown of superconductivity, i.e., the transition field between the superconducting and normal states. In case of the Fig. 1 island, the three critical fields are 0.56 ± 0.01 T, 0.51 ± 0.01 T, and 0.9 ± 0.02 T, respectively.

Field dependence of the ZBC and its images were obtained on Pb islands with different sizes and shapes as shown in Fig. 3. The radius of the island in Fig. 3(a) ($\sim$30 nm) is similar to ξ. ZBCs at the center and periphery of the island increase gradually and homogeneously with the field [17]. The gradual and homogeneous increment of ZBCs was predicted for superconducting spherical particles whose size is comparable to or smaller than ξ from a theory based on the Gor'kov equation [18]. Vortex penetration or expulsion fields decrease with the island size. The penetration fields of the island shown in Fig. 3(b), whose radius is $\sim$75 nm, are 0.38 ± 0.02 T, smaller than that of the Fig. 1 island. It should be noted that at the penetration field the ZBC at peripheral site B decreases slightly and then increases again above the field (e.g., at 0.40 T). In fact, in case of the Fig. 1 island, the gradient of the field-dependent ZBC curve [Fig. 1(d)] taken at the periphery is slightly reduced just after the vortex penetration. This can be explained with a relaxation of the penetrating magnetic field by the vortex introduction [19]. In a larger elongated island shown in Fig. 3(c), we observe the penetration of the second vortex. A ZBC image taken at 0.5 T clearly shows corresponding two peaks.

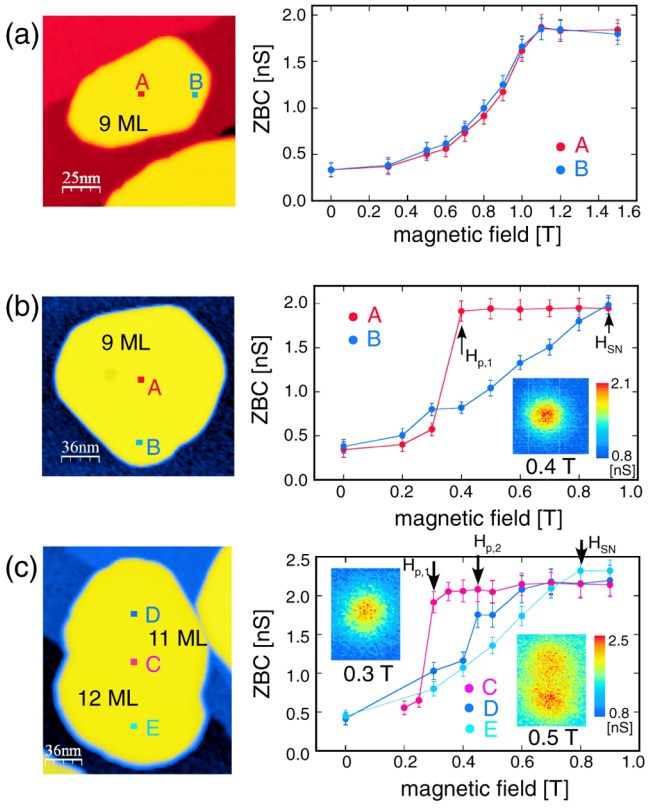

FIG. 3 (color online). ZBC plots and images obtained on Pb islands with various sizes. (a) Pb island (radius: $\sim$30 nm) smaller than that in Fig. 1. (b) Pb island (radius: $\sim$75 nm) larger than that in Fig. 1. (c) Elongated Pb island with thicknesses of 11 and 12 ML.

We measured critical fields on islands with various sizes through ZBC measurements. Figure 4 presents a plot of the fields as a function of the island radius for 9-ML-thick islands. Since the islands are not exactly circular and often show straight boundaries along the preferential crystallographic directions, the radius in this plot, r_e, is an effective one, under the assumption of circular islands, calculated using the equation $S = \pi r_e^2$, where S is the island area. The plot shows that superconductivity of islands whose radius is less than 38 nm breaks without vortex formation. The vortex is formed on islands whose radius is larger than 46 nm. Larger islands tend to have lower vortex penetration or expulsion and breakdown fields. According to theoretical studies based on linearized Ginzburg Landau (GL) equations [20,21], islands whose radius is smaller than the critical radius 1.3ξ do not form vortices. Using the critical size, ξ of the 9 ML islands at 2.0 K is estimated at 32 ± 3 nm. As the radius increases, the H_{SN} value should approach that of thin films, namely, the critical field for

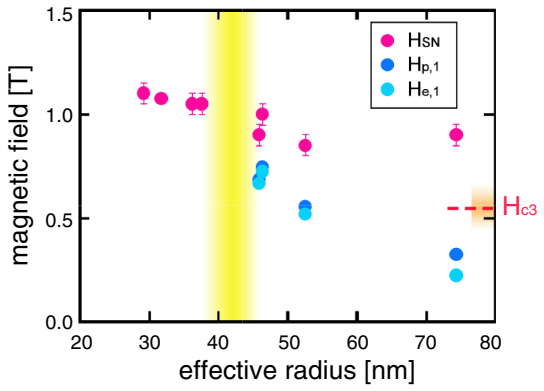

FIG. 4 (color online). Lateral size dependence of various critical fields: transition field between superconducting and normal states H_{SN}, vortex penetration H_{p1}, and vortex expulsion H_{ex1}. All critical fields were obtained on 9-ML-thickness Pb islands. The broad vertical line indicates the critical size for vortex formation.

surface superconductivity H_{c3}, which is given by $1.695 \times h/4\pi e\xi^2$, where h is Planck's constant. The range of H_{c3} calculated from the estimated ξ is shown in the plot. Using the formula $\xi(T) = \xi(0)/(1 - T/T_c)^{1/2}$, describing the temperature dependence of ξ, the coherence length at zero temperature $\xi(0)$ is obtained as 26 ± 2 nm, which is consistent with the value measured for 9 ML thin films [12]. Although this analysis neglects the effect of island shape, the experimental results are considerably consistent with those of the theoretical studies.

The calculated results of time-dependent nonlinear GL equations [22], which deal with nonequilibrated phenomena including the vortex penetration or expulsion and hysteresis, qualitatively agree with our observations. We notice, however, that the experimentally observed field differences between vortex penetration and expulsion, that is, the width of hysteresis, are significantly smaller than those expected from the GL theories. The discrepancy could originate from the noncircular shape of the islands and/or tunneling current, inevitable for STM/S, which might reduce the Bean-Livingston barrier.

Figure 4 shows critical fields only for 9 ML islands to eliminate influences of their thickness dependence. In general, thinner films have a shorter ξ because of the thickness-limited mean free path. In the case of Pb thin films, the quantum size effect on superconductivity [8] may also modulate ξ, but the estimated amount of the modulation is much smaller than the effect of the thickness-limited mean free path in our thickness range. In fact, in ZBC measurements on an island containing both 8 and 9 ML regions, we have found that the 8 ML region has a larger H_{SN} value than the 9 ML region, consistent with the relation of ξ with the thickness.

In this study, we have demonstrated magnetic field dependence and spatial distribution of superconductivity in nanosized Pb islands using STM/S. On the basis of ZBC measurements, we have obtained critical fields of vortex penetration or expulsion and breakdown for each island and discussed their size dependence based on GL equations. We believe this opens up new paths for understanding nano/mesoscopic superconductors including vortices.

We thank Akinobu Kanda for fruitful discussions and Shiro Yamazaki for tip preparation and characterization. T. N. acknowledges support by Grant-in-Aid of the Japan Society for the Promotion of Science (JSPS) for young scientists.

*Present address: PRESTO, Japan Science and Technology Agency, Chiyoda-ku, Tokyo 102-0075, Japan.
†Permanent address: Department of Materials Science and Technology, Tokyo University of Science, Noda, Chiba 278-8510, Japan.
‡Corresponding author.
hasegawa@issp.u-tokyo.ac.jp

[1] A. K. Geim *et al.*, Nature (London) **390**, 259 (1997).
[2] A. Kanda *et al.*, Phys. Rev. Lett. **93**, 257002 (2004).
[3] L. F. Chibotaru *et al.*, Nature (London) **408**, 833 (2000).
[4] H. F. Hess *et al.*, Phys. Rev. Lett. **62**, 214 (1989).
[5] H. F. Hess *et al.*, Phys. Rev. Lett. **64**, 2711 (1990).
[6] I. B. Altfeder *et al.*, Phys. Rev. Lett. **78**, 2815 (1997).
[7] W. B. Su *et al.*, Phys. Rev. Lett. **86**, 5116 (2001).
[8] Yang Guo *et al.*, Science **306**, 1915 (2004).
[9] D. Eom *et al.*, Phys. Rev. Lett. **96**, 027005 (2006).
[10] X.-Y. Bao *et al.*, Phys. Rev. Lett. **95**, 247005 (2005).
[11] T. Nishio *et al.*, Appl. Phys. Lett. **88**, 113115 (2006).
[12] M. M. Özer *et al.*, Nature Phys. **2**, 173 (2006).
[13] M. Tinkham, *Introduction of Superconductivity* (McGraw-Hill, New York, 1996), 2nd ed.
[14] Y. Kato and N. Hayashi, J. Phys. Soc. Jpn. **71**, 1721 (2002).
[15] N. Hayashi *et al.*, J. Low Temp. Phys. **139**, 79 (2005).
[16] C. P. Bean and J. D. Livingston, Phys. Rev. Lett. **12**, 14 (1964).
[17] T. Nishio *et al.*, Jpn. J. Appl. Phys. **46**, L880 (2007).
[18] S. Strässler and P. Wyder, Phys. Rev. **158**, 319 (1967).
[19] A. K. Geim *et al.*, Nature (London) **407**, 55 (2000).
[20] V. V. Moshchalkov *et al.*, Phys. Rev. B **55**, 11 793 (1997).
[21] V. A. Schweigert and F. M. Peeters, Phys. Rev. B **57**, 13 817 (1998).
[22] V. A. Schweigert and F. M. Peeters, Physica (Amsterdam) **332C**, 266 (2000).